

NAAP-440 Dataset and Baseline for Neural Architecture Accuracy Prediction

Tal Hakim

Smart Shooter, Kibbutz Yagur, Israel

tal.hakim@smart-shooter.com

Abstract

Neural architecture search (NAS) has become a common approach to developing and discovering new neural architectures for different target platforms and purposes. However, scanning the search space is comprised of long training processes of many candidate architectures, which is costly in terms of computational resources and time. Regression algorithms are a common tool to predicting a candidate architecture’s accuracy, which can dramatically accelerate the search procedure. We aim at proposing a new baseline that will support the development of regression algorithms that can predict an architecture’s accuracy just from its scheme, or by only training it for a minimal number of epochs. Therefore, we introduce the NAAP-440 dataset of 440 neural architectures, which were trained on CIFAR10 using a fixed recipe. Our experiments indicate that by using off-the-shelf regression algorithms and running up to 10% of the training process, not only is it possible to predict an architecture’s accuracy rather precisely, but that the values predicted for the architectures also maintain their accuracy order with a minimal number of monotonicity violations. This approach may serve as a powerful tool for accelerating NAS-based studies and thus dramatically increase their efficiency. The dataset ¹ and code used in the study ² have been made public.

1. Introduction

Over the recent decade, convolutional neural networks have been evolving and improving in their accuracy and efficiency [4, 6, 7, 11, 19, 21, 22, 28], with the development of new ideas and approaches, such as batch normalization [8], residual blocks [4], inverted residual blocks [19], grouped convolutions [28], squeeze-and-excitation blocks [6] and many others. In the recent years, a leading approach for discovering new architectures is Neural Architecture Search (NAS) [5, 23–25, 33, 34] and other NAS-inspired ap-

¹<https://www.kaggle.com/datasets/talcs1/naap-440>

²<https://github.com/talcs/NAAP-440>

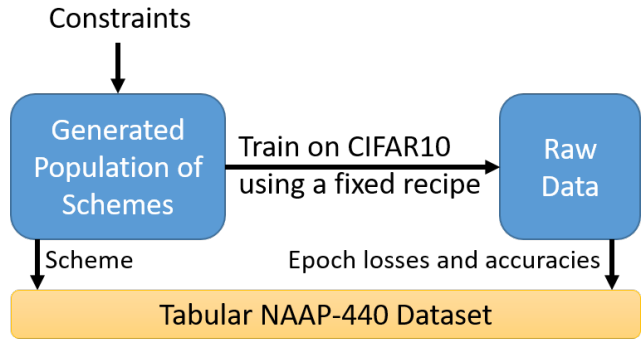


Figure 1. The creation of the dataset starts with defining a population of neural architectures. All the architectures are trained using the same fixed recipe and are evaluated on CIFAR10 test set after every epoch. The NAAP-440 dataset is formed from the collected data.

proaches [12, 18], in the sense that they are based on a massive experimentation with many candidate architectures.

The main drawback of the NAS approach is its resource consumption, which for instance, could be 500 GPUs running for 4 days [34]. While it is a rather trivial and inexpensive task to evaluate a candidate architecture in terms of efficiency, by counting MACs or measuring its runtime on a single batch [23–25], it is a rather expensive task to compute the architecture’s accuracy, as it requires training it first using a given recipe.

The idea of predicting an architecture’s accuracy has already been studied [1, 9, 13, 16, 32]. The NAS-Bench-101 [30], NAS-Bench-201 [2] and NAS-Bench-301 [20] datasets of neural architectures and their corresponding accuracies have been published over the years, which have been extensively used for designing regression algorithms that are intended for accelerating the search process, as well as evaluating search techniques [3, 15, 26, 27, 29, 31].

We aim at introducing a new baseline for developing regression algorithms and a set of features that will allow for correctly predicting a candidate architecture’s accuracy with a minimal cost of resources. By saving 90% up to 100% of an architecture’s training time, we anticipate that

our approach will join the efforts to make NAS dramatically more efficient, which will allow for the scan of wider search spaces and thus the discovery of better architectures.

For that purpose, we introduce the NAAP-440 dataset, which consists of 440 neural architectures trained and evaluated on the CIFAR10 dataset [10]. As visualized in Figure 1, we generate 440 neural architectures using a set of constraints and use a fixed training recipe to train each of them. After each epoch, we document the value of the loss function and evaluate the model on the CIFAR10 test set. As a result, our dataset contains both scheme features and features from the training process. We evenly sample 40 architectures, to form a training set of 400 architectures and a test set of 40 architectures. Our aim is that, given a minimal number of features from the training epochs, to predict an architecture’s highest accuracy score achieved on the CIFAR10 test set, over all its training epochs. We perform ablation studies on the feature set and provide a baseline of performance reports using many regression algorithms and combinations of features. We measure the quality of the accuracy prediction using two measures: mean absolute error and monotonicity score.

Our experiments indicate that by using off-the-shelf regression algorithms, it is actually possible not to train the architectures on CIFAR10 at all, or in other words, to accelerate the training process by 100%, and still predict their CIFAR10 test set accuracy scores with MAE of 0.5% and only 42 monotonicity violations, out of $\binom{40}{2} = 780$ possible violations. Furthermore, the experiments indicate that by only training each architecture on CIFAR10 for 10% of the epochs and evaluating them after every epoch, or in other words, accelerating the training process by 90%, it is possible to predict their CIFAR10 test set accuracy scores with MAE of 0.4% and only 25 monotonicity violations, as demonstrated in Figures 5,6 and Table 3. We believe that using this approach, it will be possible to accelerate any NAS-based solution, by building similar regression algorithms using a rather small population of architectures sampled from the search space, then using the regression algorithms for the whole search space.

Our contributions in this study are as follows. First, we create the NAAP-440 dataset and make it public for further research. Second, we conduct ablation studies and experiments that form a baseline of performances to be used as a reference. Third, we introduce the monotonicity-based evaluation and show that evaluating candidate architectures can be accelerated by up to 100% and still be accurate.

We encourage researchers to use the NAAP-440 dataset in their studies and try to improve it from any aspect, including improving the reported baseline results, extending the evaluation metrics and extending the dataset.

2. Dataset

Scheme Generation. The schemes are generated using a DFS scan on the convolutional layers with a set of constraints. As visualized in Figure 2, some constraints are imposed on the whole model, while others are imposed per layer. For the model itself, the number of convolutional layers varies between 3 and 4 and the number of stages varies between 2 and 3. The layers themselves can vary in their kernel size, width, stride and whether they have a skip connection. Every convolutional layer is followed by batch normalization [8] and ReLU. We always use convolutional layers with no bias and with padding of $\lfloor \frac{S}{2} \rfloor$, where S is the kernel size. Since layers 1,2 are fixed to have stride=2, only up to one of layers 3,4 can be assigned with stride=2, to enforce the number of stages varying between 2 and 3. A skip connection can be applied only if the layer’s input shape agrees with its output shape, which can only occur when the stride is selected to be 1 and the width of the current layer is equal to the width of the previous layer. The total number of valid schemes according to our set of constraints is 440.

Architecture Training. In order to generate the dataset, we turn the 440 schemes into actual architectures and train each of them on the CIFAR10 dataset for 90 epochs. For reproducibility, we initialize a fixed random-seed before initializing each model’s weights and before initializing the shuffled training set loader, as well as switching the accelerators to deterministic mode. This ensures that all the architectures are trained using the same permutation of the training set. We use CE loss and the SGD optimizer with warm restarts [14] every 3 epochs. The training recipe is as follows: batch-size: 256, momentum: 0.9, weight-decay: 0.0001, learning-rate: 0.1, with exponential decay, by multiplying by 0.1 after every epoch. As the whole training runs for 90 epochs and the learning rate restarts after every 3 epochs, the process can be described as a sequence of 30 training cycles, each consisting of 3 epochs.

Dataset Structure. We build a tabular dataset that contains all the 440 architectures. Each architecture is reported with its scheme details and the collected data from its training and evaluation on CIFAR10. The scheme details include the network’s depth, number of stages, first and last layer widths, number of total parameters and number of total MACs. The data from the training and evaluation on CIFAR10 is provided for each of the 90 epochs and includes the model’s accuracy on CIFAR10 test set after each epoch is completed, as well as each epoch’s mean and median training loss over all the SGD batches.

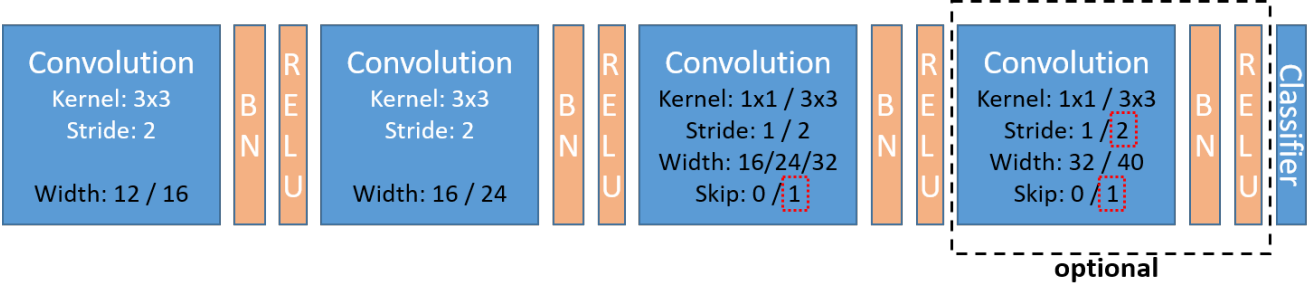


Figure 2. The set of constraints that define the population of network schemes that form the dataset. A red dotted rectangle denotes an assignment that is only possible under certain conditions: skip is only possible if a layer’s input and output shapes match, stride=2 at the forth layer is only possible if the third layer has been assigned with stride=1, as the number of stages has been defined to be 2 or 3.

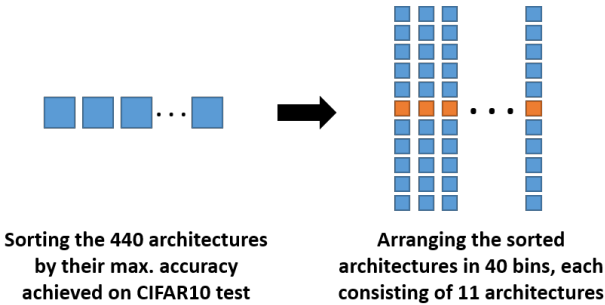


Figure 3. Division of the NAAP-440 dataset into train and test sets. The architectures at the central index of each bin are allocated to the test set.

Separating into Train and Test Sets. We would like to create a fair separation of the 440 architecture data records into train and test sets. Our first choice deals with quantities - we would like to allocate 400 samples to the training set and 40 samples to the test set. The second and more complicated choice is how to select the 40 test samples in a deterministic and even way, in terms of the network structure and performances. The original order of the architectures has been determined by the DFS scan over the set of constraints, which we consider unsatisfactory. Instead, as visualized in Figure 3, we sort the architectures by their accuracy scores on the CIFAR10 test set, using the highest achieved score over all the training epochs. Then, we arrange the 440 architectures in 40 bins, such that each bin consists of 11 architectures that have similar accuracy scores on the CIFAR10 test set. From each bin, we allocate the architecture at the central index to the test set. This deterministic operation leaves us with 400 training samples and 40 representative test samples.

3. Evaluation Metrics

Prediction Accuracy. In order to evaluate the quality of a proposed regression model, we use multiple measures.



Figure 4. A sequence of seven items ordered with a single misplaced item, causing three violations of monotonicity. The maximum number of violations possible is the number of unordered pairs, which is equal to $\binom{7}{2} = 21$ in this example. The monotonicity score of this example will therefore be $1 - \frac{3}{21} = \frac{6}{7}$

The first and rather obvious one is the Mean Absolute Error (MAE) metric, which reflects the overall quality of the regression model.

Monotonicity Score. Being able to compare two candidate architectures to each other is an important capability when searching for neural architectures. Using a regression model’s predicted accuracy of the two architectures can serve as a measure for comparison. However, while some proposed regression models might provide accurate predictions for most of the test samples, their predictions are not guaranteed to preserve the original order of the samples, which may lead to a misleading comparison. For that reason, another metric that we propose is a monotonicity score. As visualized in Figure 4, given N samples, the maximum possible number of monotonicity violations, is the number of pairs, which is $\binom{N}{2} = N(N-1)/2$. Therefore, the monotonicity score we propose is

$$1 - \frac{\#violations}{\binom{N}{2}}, \tag{1}$$

while in our case, $N = 40$, such that $\binom{N}{2} = 780$. Thus, the monotonicity score will be equal to 1 when the predictions maintain the order of the architecture accuracies perfectly. In contrast, it will be equal to 0 when the predictions result in an exactly reversed version of the original order of the architecture accuracies, a situation where every pairwise

Feature Set	MAE	#Violations
All but NumMACs	0.0071	50
All but Depth	0.0078	57
All but LastLayerWidth	0.0077	57
All but FirstLayerWidth	0.008	58
All	0.0079	60
All but NumStages	0.0134	81
All but LogNumParams	0.0199	111
LogNumParams & NumStages	0.0063	48

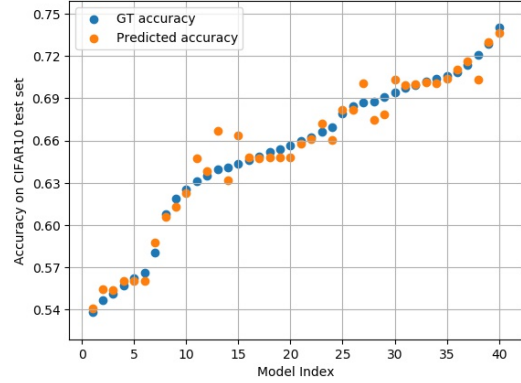
Table 1. Ablation study on the scheme features using Random Forest regressor with N=200 trees. When only using scheme features (without any features from the training process), the LogNumParams and NumStages features are the most essential ones, while others do not contribute to, or even harm the performance.

Training Length	0 Scheme Features	2 Scheme Features	6 Scheme Features
0 epochs	-	48	60
3 epochs	110	35	32
6 epochs	95	30	25
9 epochs	78	37	25
12 epochs	72	41	27
15 epochs	56	42	29
18 epochs	63	51	44

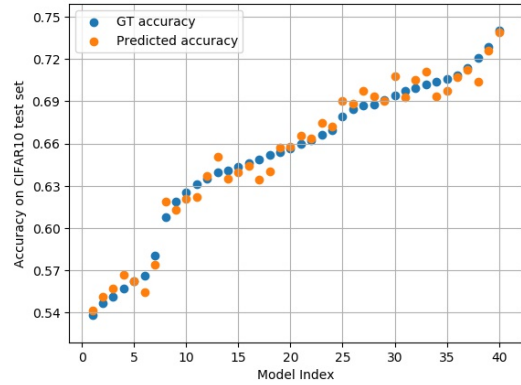
Table 2. Ablation study on the scheme features when combining features from the initial epochs of the architectures’ training processes on CIFAR10, using Random Forest regressor with N=200 trees. The values reported on the table are the number of monotonicity violations made by the regression model. The subset of 2 scheme features is only preferable when using no features from the training process.

comparison of architectures using the regression model will be incorrect.

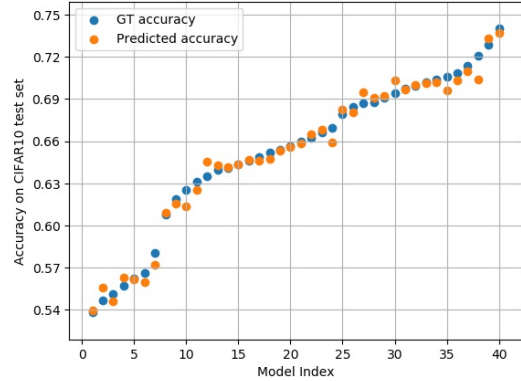
Search Acceleration. The architecture accuracy prediction can be performed under different conditions. Since our aim is to predict the highest test accuracy on CIFAR10 in the course of 90 training epochs, a regression model that only uses an architecture’s details from the 9 first epochs, which are 10% of the training process, accelerates the search by 90%. Similarly, a regression model that only uses the schematic features accelerates the search by 100%, as it requires no training at all. We therefore evaluate different regression algorithms on the dataset under different feature sets, to emphasize the trade-off between search acceleration, prediction accuracy and prediction monotonicity.



(a) Using Gradient Boosting (N=100 estimators) and only scheme features as input, MAE=0.006.



(b) Using Linear Regression (D=0.5), using scheme and 9 epoch features as input, MAE=0.006.



(c) Using Random Forest (N=200 trees), using scheme and 9 epoch features as input, MAE=0.004.

Figure 5. Accuracy prediction results on the NAAP-440 test set.

4. Evaluation Baseline

Scheme Features Ablation Study. As described in Section 2, the dataset’s schematic details include 6 features, which are the network’s depth, number of stages, first and last layer widths, number of total parameters and number of total MACs. We aim at checking whether all of the scheme

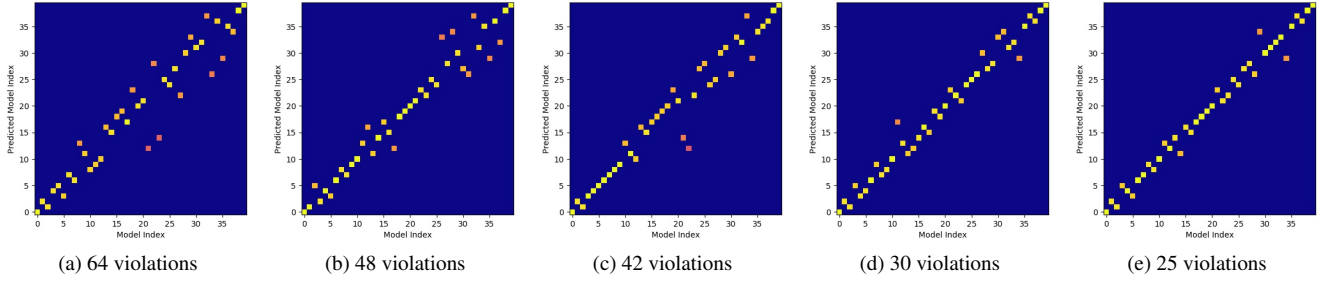


Figure 6. Visualized monotonicity of accuracies predicted by: (a) linear regression only using scheme features, (b) linear regression using scheme features and features from 9 training epochs, (c) Gradient Boosting (N=100 estimators) only using scheme features, (d) SVR (RBF kernel) using scheme features and features from 6 training epochs, (e) Random Forest (N=200 estimators) using scheme features and features from 9 training epochs.

Algorithm	MAE / Monotonicity Score / #Monotonicity Violations			
	100.0% acceleration (0 epochs)	96.7% acceleration (3 epochs)	93.3% acceleration (6 epochs)	90.0% acceleration (9 epochs)
1-NN	0.007 / 0.933 / 52	0.009 / 0.929 / 55	0.007 / 0.940 / 47	0.006 / 0.959 / 32
3-NN	0.009 / 0.918 / 64	0.007 / 0.944 / 44	0.007 / 0.950 / 39	0.007 / 0.951 / 38
5-NN	0.010 / 0.908 / 72	0.008 / 0.942 / 45	0.007 / 0.941 / 46	0.007 / 0.949 / 40
7-NN	0.009 / 0.909 / 71	0.007 / 0.950 / 39	0.007 / 0.951 / 38	0.006 / 0.962 / 30
9-NN	0.010 / 0.914 / 67	0.009 / 0.942 / 45	0.007 / 0.960 / 31	0.007 / 0.951 / 38
Linear Regression	0.017 / 0.918 / 64	0.009 / 0.926 / 58	0.008 / 0.941 / 46	0.007 / 0.942 / 45
Linear Regression (D=0.5)	0.015 / 0.919 / 63	0.008 / 0.932 / 53	0.007 / 0.942 / 45	0.006 / 0.947 / 41
Linear Regression (D=0.25)	0.013 / 0.919 / 63	0.008 / 0.935 / 51	0.007 / 0.942 / 45	0.006 / 0.947 / 41
Decision Tree	0.007 / 0.931 / 54	0.007 / 0.929 / 55	0.008 / 0.924 / 59	0.007 / 0.933 / 52
Gradient Boosting (N=25)	0.009 / 0.944 / 44	0.008 / 0.953 / 37	0.006 / 0.951 / 38	0.006 / 0.958 / 33
Gradient Boosting (N=50)	0.007 / 0.940 / 47	0.006 / 0.955 / 35	0.006 / 0.953 / 37	0.005 / 0.956 / 34
Gradient Boosting (N=100)	0.006 / 0.946 / 42	0.006 / 0.958 / 33	0.006 / 0.960 / 31	0.006 / 0.959 / 32
Gradient Boosting (N=200)	0.005 / 0.945 / 43	0.006 / 0.951 / 38	0.006 / 0.962 / 30	0.006 / 0.958 / 33
AdaBoost (N=25)	0.010 / 0.933 / 52	0.009 / 0.947 / 41	0.007 / 0.953 / 37	0.006 / 0.955 / 35
AdaBoost (N=50)	0.010 / 0.933 / 52	0.008 / 0.945 / 43	0.006 / 0.953 / 37	0.006 / 0.958 / 33
AdaBoost (N=100)	0.010 / 0.933 / 52	0.008 / 0.944 / 44	0.007 / 0.951 / 38	0.005 / 0.955 / 35
AdaBoost (N=200)	0.010 / 0.933 / 52	0.008 / 0.944 / 44	0.007 / 0.951 / 38	0.006 / 0.954 / 36
SVR (RBF kernel)	0.009 / 0.913 / 68	0.007 / 0.949 / 40	0.005 / 0.962 / 30	0.005 / 0.960 / 31
SVR (Polynomial kernel)	0.020 / 0.911 / 69	0.008 / 0.940 / 47	0.009 / 0.919 / 63	0.010 / 0.918 / 64
SVR (Linear kernel)	0.017 / 0.917 / 65	0.009 / 0.933 / 52	0.008 / 0.944 / 44	0.007 / 0.947 / 41
Random Forest (N=25)	0.007 / 0.935 / 51	0.006 / 0.954 / 36	0.005 / 0.958 / 33	0.004 / 0.964 / 28
Random Forest (N=50)	0.006 / 0.936 / 50	0.006 / 0.956 / 34	0.005 / 0.963 / 29	0.005 / 0.964 / 28
Random Forest (N=100)	0.006 / 0.939 / 48	0.005 / 0.956 / 34	0.005 / 0.967 / 26	0.004 / 0.965 / 27
Random Forest (N=200)	0.006 / 0.939 / 48	0.005 / 0.959 / 32	0.005 / 0.968 / 25	0.004 / 0.968 / 25

Table 3. Baseline results using various regression algorithms. For linear regression with a specified degree D, the model is trained to predict $y = (\vec{w} \cdot \vec{x} + 1)^D$ rather than $y = \vec{w} \cdot \vec{x}$. It is achieved by training the model to predict $y^{1/D} - 1$. All ensemble regressors are specified with their number of estimators, N.

features are essential to training a regression model. We were surprised to witness most of the scheme features actually harming the regression accuracy repeatedly, under different regression algorithms, including Random Forest, Gradient Boosting and Linear Regression. Table 1 demonstrates that that number of parameters and number of stages

are most essential for an accurate regression, as removing them from the feature set causes a notable degradation. On the other hand, the removal of each of the other features actually contributes to the regressor performance, when using a Random Forest regressor. However, when we do combine the features from the training process, which as described

in Section 2, include each epoch’s accuracy on CIFAR10 test set as well as its mean and median loss on the training set, we observe that the complete set of scheme features is essential. Table 2 shows the essence of the complete set of scheme features when features from the training process are included. Furthermore, when using a linear regression model, we find it very essential to use a logarithmic version of the number-of-parameters feature. When only using scheme features, it reduces the trained regression model’s number of monotonicity violations from 89 to 64 and the MAE from 2.3% to 1.7%. To conclude, we recommend to apply the logarithmic function on the number-of-parameters feature, to only use the limited set of scheme features when choosing not to train the model at all and to keep using all 6 scheme features when including features from the training process.

Baseline. After we have understood the effect and contribution of each feature to the performance of the regressor, we proceed to providing a baseline using many regression algorithms under different settings in Table 3. We used the scikit-learn [17] Python package for that purpose. Since some of the regression algorithms have different performances under different random seeds, we repeat running each algorithm 5 times using different seeds and report their median performance, according to the number of violations. As guided by the ablation studies, we use the limited scheme feature set when not using features from the training epochs, while using all the scheme features when we do use features from the training epochs. Furthermore, we exclude results when using features of more than 9 training epochs, since as demonstrated in Table 2, we observe that features from further training epochs usually do not contribute to and even harm the performance. Figures 5,6 demonstrate the strengths of different regression algorithms with different feature sets. In all the experiments conducted, all features are fed to the regressors after scale and bias normalization, which is learned from the training set.

Naive Reference. As a reference for the regression algorithms, we report that the MAE achieved by a dummy regressor, which always outputs the mean of the training set, is 0.043. As all architectures are predicted with the same accuracy, their prediction-based order is equivalent to any random permutation. It should be possible to prove that the average number of violations over all permutations is identically $\frac{1}{2} \binom{N}{2}$. We check 500 random permutations of the 40 architectures, and as we expect, we observe that their average number of monotonicity violations is $390 = \frac{1}{2} \binom{40}{2}$, which results in a monotonicity score of exactly 0.5. Therefore, a reasonable regressor should achieve MAE < 0.043 and less than 390 monotonicity violations on the NAAP-440 test set. The naive reference emphasizes the importance of

using the monotonicity score alongside the MAE metric.

5. Conclusions and Future Work

We have presented the NAAP-440 dataset for architecture accuracy prediction, which includes 440 scheme-generated neural architectures trained and evaluated on the CIFAR10 dataset. Our experiments show that by accelerating the training process by up to 100%, it is possible to predict an architecture’s accuracy score quite precisely, as well as maintain the 40 test architecture’s accuracy-based order with a quite a low number of violations. As we have published the dataset and the code, we hope that the dataset will be used by other researchers to improve and push the boundaries of neural architecture accuracy prediction capabilities.

For future work, we may consider (1) examining additional train/test divisions that may require the usage of regression algorithms that can extrapolate, (2) enriching the dataset with more architectures, (3) creating another dataset that will have a fixed architecture and variable training recipes, as opposed to this work’s fixed training recipe and variable architectures.

References

- [1] Bowen Baker, Otakrist Gupta, Ramesh Raskar, and Nikhil Naik. Practical neural network performance prediction for early stopping. *arXiv preprint arXiv:1705.10823*, 2(3):6, 2017. 1
- [2] Xuanyi Dong and Yi Yang. Nas-bench-201: Extending the scope of reproducible neural architecture search. *arXiv preprint arXiv:2001.00326*, 2020. 1
- [3] Ekaterina Gracheva. Trainless model performance estimation based on random weights initialisations for neural architecture search. *Array*, 12:100082, 2021. 1
- [4] Kaiming He, Xiangyu Zhang, Shaoqing Ren, and Jian Sun. Deep residual learning for image recognition. In *Proceedings of the IEEE conference on computer vision and pattern recognition*, pages 770–778, 2016. 1
- [5] Andrew Howard, Mark Sandler, Grace Chu, Liang-Chieh Chen, Bo Chen, Mingxing Tan, Weijun Wang, Yukun Zhu, Ruoming Pang, Vijay Vasudevan, et al. Searching for mobilenetv3. In *Proceedings of the IEEE/CVF international conference on computer vision*, pages 1314–1324, 2019. 1
- [6] Jie Hu, Li Shen, and Gang Sun. Squeeze-and-excitation networks. In *Proceedings of the IEEE conference on computer vision and pattern recognition*, pages 7132–7141, 2018. 1
- [7] Gao Huang, Zhuang Liu, Laurens Van Der Maaten, and Kilian Q Weinberger. Densely connected convolutional networks. In *Proceedings of the IEEE conference on computer vision and pattern recognition*, pages 4700–4708, 2017. 1
- [8] Sergey Ioffe and Christian Szegedy. Batch normalization: Accelerating deep network training by reducing internal covariate shift. In *International conference on machine learning*, pages 448–456. PMLR, 2015. 1, 2

- [9] Roxana Istrate, Florian Scheidegger, Giovanni Mariani, Dimitrios Nikolopoulos, Constantine Bekas, and Adelmo Cristiano Innocenza Malossi. Tapas: Train-less accuracy predictor for architecture search. In *Proceedings of the AAAI Conference on Artificial Intelligence*, volume 33, pages 3927–3934, 2019. 1
- [10] Alex Krizhevsky, Geoffrey Hinton, et al. Learning multiple layers of features from tiny images. 2009. 2
- [11] Alex Krizhevsky, Ilya Sutskever, and Geoffrey E Hinton. Imagenet classification with deep convolutional neural networks. *Communications of the ACM*, 60(6):84–90, 2017. 1
- [12] Zhuang Liu, Hanzi Mao, Chao-Yuan Wu, Christoph Feichtenhofer, Trevor Darrell, and Saining Xie. A convnet for the 2020s. In *Proceedings of the IEEE/CVF Conference on Computer Vision and Pattern Recognition*, pages 11976–11986, 2022. 1
- [13] Duo Long, Shizhou Zhang, and Yanning Zhang. Performance prediction based on neural architecture features. *Cognitive Computation and Systems*, 2(2):80–83, 2020. 1
- [14] Ilya Loshchilov and Frank Hutter. Sgdr: Stochastic gradient descent with warm restarts. *arXiv preprint arXiv:1608.03983*, 2016. 2
- [15] Renqian Luo, Xu Tan, Rui Wang, Tao Qin, Enhong Chen, and Tie-Yan Liu. Accuracy prediction with non-neural model for neural architecture search. *arXiv preprint arXiv:2007.04785*, 2020. 1
- [16] Joe Mellor, Jack Turner, Amos Storkey, and Elliot J Crowley. Neural architecture search without training. In *International Conference on Machine Learning*, pages 7588–7598. PMLR, 2021. 1
- [17] F. Pedregosa, G. Varoquaux, A. Gramfort, V. Michel, B. Thirion, O. Grisel, M. Blondel, P. Prettenhofer, R. Weiss, V. Dubourg, J. Vanderplas, A. Passos, D. Cournapeau, M. Brucher, M. Perrot, and E. Duchesnay. Scikit-learn: Machine learning in Python. *Journal of Machine Learning Research*, 12:2825–2830, 2011. 6
- [18] Ilija Radosavovic, Raj Prateek Kosaraju, Ross Girshick, Kaifeng He, and Piotr Dollár. Designing network design spaces. In *Proceedings of the IEEE/CVF conference on computer vision and pattern recognition*, pages 10428–10436, 2020. 1
- [19] Mark Sandler, Andrew Howard, Menglong Zhu, Andrey Zhmoginov, and Liang-Chieh Chen. Mobilenetv2: Inverted residuals and linear bottlenecks. In *Proceedings of the IEEE conference on computer vision and pattern recognition*, pages 4510–4520, 2018. 1
- [20] Julien Siems, Lucas Zimmer, Arber Zela, Jovita Lukasik, Margret Keuper, and Frank Hutter. Nas-bench-301 and the case for surrogate benchmarks for neural architecture search. *arXiv preprint arXiv:2008.09777*, 2020. 1
- [21] Karen Simonyan and Andrew Zisserman. Very deep convolutional networks for large-scale image recognition. *arXiv preprint arXiv:1409.1556*, 2014. 1
- [22] Christian Szegedy, Vincent Vanhoucke, Sergey Ioffe, Jon Shlens, and Zbigniew Wojna. Rethinking the inception architecture for computer vision. In *Proceedings of the IEEE conference on computer vision and pattern recognition*, pages 2818–2826, 2016. 1
- [23] Mingxing Tan, Bo Chen, Ruoming Pang, Vijay Vasudevan, Mark Sandler, Andrew Howard, and Quoc V Le. Mnasnet: Platform-aware neural architecture search for mobile. In *Proceedings of the IEEE/CVF Conference on Computer Vision and Pattern Recognition*, pages 2820–2828, 2019. 1
- [24] Mingxing Tan and Quoc Le. Efficientnet: Rethinking model scaling for convolutional neural networks. In *International conference on machine learning*, pages 6105–6114. PMLR, 2019. 1
- [25] Mingxing Tan and Quoc Le. Efficientnetv2: Smaller models and faster training. In *International Conference on Machine Learning*, pages 10096–10106. PMLR, 2021. 1
- [26] Wei Wen, Hanxiao Liu, Yiran Chen, Hai Li, Gabriel Bender, and Pieter-Jan Kindermans. Neural predictor for neural architecture search. In *European Conference on Computer Vision*, pages 660–676. Springer, 2020. 1
- [27] Colin White, Arber Zela, Robin Ru, Yang Liu, and Frank Hutter. How powerful are performance predictors in neural architecture search? *Advances in Neural Information Processing Systems*, 34:28454–28469, 2021. 1
- [28] Saining Xie, Ross Girshick, Piotr Dollár, Zhuowen Tu, and Kaifeng He. Aggregated residual transformations for deep neural networks. In *Proceedings of the IEEE conference on computer vision and pattern recognition*, pages 1492–1500, 2017. 1
- [29] Yixing Xu, Yunhe Wang, Kai Han, Yehui Tang, Shangling Jui, Chunjing Xu, and Chang Xu. Renas: Relativistic evaluation of neural architecture search. In *Proceedings of the IEEE/CVF Conference on Computer Vision and Pattern Recognition*, pages 4411–4420, 2021. 1
- [30] Chris Ying, Aaron Klein, Eric Christiansen, Esteban Real, Kevin Murphy, and Frank Hutter. Nas-bench-101: Towards reproducible neural architecture search. In *International Conference on Machine Learning*, pages 7105–7114. PMLR, 2019. 1
- [31] Arber Zela, Julien Siems, and Frank Hutter. Nas-bench-1shot1: Benchmarking and dissecting one-shot neural architecture search. *arXiv preprint arXiv:2001.10422*, 2020. 1
- [32] Meili Zhou, Zongwen Bai, Tingting Yi, Xiaohuan Chen, and Wei Wei. Performance predict method based on neural architecture search. *Journal of Internet Technology*, 21(2):385–392, 2020. 1
- [33] Barret Zoph and Quoc V Le. Neural architecture search with reinforcement learning. *arXiv preprint arXiv:1611.01578*, 2016. 1
- [34] Barret Zoph, Vijay Vasudevan, Jonathon Shlens, and Quoc V Le. Learning transferable architectures for scalable image recognition. In *Proceedings of the IEEE conference on computer vision and pattern recognition*, pages 8697–8710, 2018. 1